Targeting mitochondrial dysfunction using methylene blue or mitoquinone to improve skeletal aging

Sher Bahadur Poudel[1], Dorra Frikha-Benayed[2], Ryan R. Ruff[3], Gozde Yildirim[1], Manisha Dixit[1], Ron Korstanje[4], Laura Robinson[4], Richard A. Miller[5], David E. Harrison[6], John R. Strong[7,8], Mitchell B. Schaffler[2], Shoshana Yakar[1]

[1]Department of Molecular Pathobiology, David B. Kriser Dental Center, New York University College of Dentistry, New York, NY 10010-4086, USA
[2]Department of Biomedical Engineering, City College of New York, New York, NY 10031, USA
[3]Department of Epidemiology and Health Promotion, David B. Kriser Dental Center, New York University College of Dentistry, New York, NY 10010-4086, USA
[4]Jackson Aging Center, Nathan Shock Center for Excellence in the Basic Biology of Aging, The Jackson's Laboratories, Aging Center, Bar Harbor, ME 04609, USA
[5]Department of Pathology and Geriatrics Center, University of Michigan, Ann Arbor, MI 48109, USA
[6]The Jackson Laboratory, Bar Harbor, ME 04609, USA
[7]Geriatric Research, Education and Clinical Center and Research Service, South Texas Veterans Health Care System, San Antonio, TX 78229, USA
[8]Department of Pharmacology, Barshop Institute for Longevity and Aging Studies, The University of Texas Health Science Center, San Antonio, TX 78229, USA

Correspondence to: Shoshana Yakar; **email:** sy1007@nyu.edu

ABSTRACT

Methylene blue (MB) is a well-established antioxidant that has been shown to improve mitochondrial function in both *in vitro* and *in vivo* settings. Mitoquinone (MitoQ) is a selective antioxidant that specifically targets mitochondria and effectively reduces the accumulation of reactive oxygen species.

To investigate the effect of long-term administration of MB on skeletal morphology, we administered MB to aged (18 months old) female C57BL/J6 mice, as well as to adult male and female mice with a genetically diverse background (UM-HET3). Additionally, we used MitoQ as an alternative approach to target mitochondrial oxidative stress during aging in adult female and male UM-HET3 mice.

Although we observed some beneficial effects of MB and MitoQ *in vitro*, the administration of these compounds *in vivo* did not alter the progression of age-induced bone loss. Specifically, treating 18-month-old female mice with MB for 6 or 12 months did not have an effect on age-related bone loss. Similarly, long-term treatment with MB from 7 to 22 months or with MitoQ from 4 to 22 months of age did not affect the morphology of cortical bone at the mid-diaphysis of the femur, trabecular bone at the distal-metaphysis of the femur, or trabecular bone at the lumbar vertebra-5 in UM-HET3 mice.

Based on our findings, it appears that long-term treatment with MB or MitoQ alone, as a means to reduce skeletal oxidative stress, is insufficient to inhibit age-associated bone loss. This supports the notion that interventions solely with antioxidants may not provide adequate protection against skeletal aging.

INTRODUCTION

The existing literature supports the notion that oxidative stress and mitochondrial dysfunction are contributors to impaired skeletal aging. This concept is affirmed by randomized clinical studies (summarized in [1]), which have shown a correlation between consumption of an antioxidant-rich diet and risk of osteoporosis [2, 3]. Furthermore, a study of postmenopausal women with osteoporosis revealed decreased activity of the antioxidant enzyme glutathione reductase in serum in comparison to non-osteoporotic postmenopausal women, as well as increased plasma levels of the oxidative stress marker, malondialdehyde [4]. In addition, a range of *in vitro* and *in vivo* animal studies (reviewed in [5, 6]) have revealed a negative association between oxidative stress and bone mineral density (BMD). *In vitro* studies show that H_2O_2-induced oxidative stress adversely affected the proliferation, differentiation, and mineralization of rat primary osteoblast cultures, yet the effects were partially alleviated by supplementation with the antioxidant amino acid derivative, N-acetyl cysteine (NAC) [7]. Overall, it appears that disruptions in redox homeostasis have a detrimental impact on bone cell differentiation, function, and overall skeletal health. As a result, there is a growing interest in exploring the potential prophylactic use of antioxidants as a means to prevent osteoporosis and age-related bone loss.

Methylene blue (MB) is an FDA-approved medication that has been widely used in clinical practice for over a century. At the cellular level, MB exhibits a notable ability to traverse the cell membrane, distributing itself across various subcellular compartments such as lysosomes and mitochondria [8–10]. MB's affinity for mitochondria appears particularly significant. Numerous studies suggest that its hydrophilic/lipophilic properties and positive charge contribute to its accumulation within mitochondria, driven by the mitochondrial membrane potential [11]. MB has a low redox potential, and in the presence of molecular oxygen, the reduced form of MB (MBH_2) bypasses the production of harmful superoxide radicals. Instead, it enhances the efficiency of the Electron Transport Chain (ETC) by increasing the activity of mitochondrial complex IV. This leads to improved mitochondrial function and helps maintain the integrity of these crucial cellular structures (Figure 1A).

Previous studies have demonstrated various beneficial effects of MB. MB led to significant increase in "maximal lifespan" (proportion of mice alive at the 90th percentile) of genetically diverse UM-HET3 female mice [12]. It has been shown to improve memory function in aging individuals [13–16] and has the potential to counteract cognitive impairments associated with conditions such as Alzheimer's disease. MB can also inhibit the production of amyloid-beta, a protein implicated in Alzheimer's pathology, and rescue cognitive defects [17, 18]. Additionally, MB has been found to promote wound healing [19], stimulate the proliferation of skin cells, and reduce markers of aging in the skin [20, 21]. Notably, MB has shown promise in the treatment of Hutchinson-Gilford Progeria Syndrome (HGPS), a genetic disorder that is in some respects a model of accelerated aging [22]. Several studies have indicated that MB elicits positive effects on the skeleton. The combination of MB and low-level laser therapy (LLLT) significantly increased bone modeling in a femoral bone defect model. The combined therapy also enhanced radiopacity, suggesting improved bone healing. The study suggests that MB with LLLT may stimulate bone repair and could be beneficial for bone healing [23]. Using a rat model of osteoarthritis (OA), intra-articular MB injections significantly inhibited synovitis (inflammation), relieved pain, and prevented cartilage degradation. *In vitro* experiments using human chondrocytes and fibroblast-like synoviocytes demonstrated that MB attenuated oxidative stress and inflammation induced by tert-butyl hydroperoxide. The study highlights the potential of MB as an antioxidant agent for preventing OA progression and relieving pain [24]. Finally, *in vitro* experiments using THP-1 macrophages showed that MB-mediated photo-dynamic therapy (MB-PDT) induced macrophage apoptosis through reactive oxygen species (ROS) and the mitochondrial-dependent apoptotic pathway. *In vivo* experiments in rats with periodontitis revealed that MB-PDT led to fewer infiltrated macrophages, reduced bone loss, and lower levels of inflammatory markers compared to control treatments [25].

Mitoquinone (MitoQ) is an antioxidant that targets mitochondria. It is a lipophilic conjugated compound that has the ability to accumulate in high concentrations within the mitochondria (Figure 1A). Once inside the mitochondria, MitoQ activates ubiquinone oxido-reductases, which are enzymes involved in the electron transport chain. This activation leads to the reduction of ubiquinone to its active antioxidant form called ubiquinol [26].

The administration of MitoQ did not result in a significant effect on lifespan when tested in UM-HET3 mice [12]; however, evidence from several studies suggests that MitoQ is beneficial for bone health. In db/db mice and in mice fed a high-fat diet, MitoQ was found to inhibit bone loss. Additionally, *in vitro* studies using bone marrow stromal cells from db/db mice showed that MitoQ significantly improved osteogenic

differentiation. This improvement was associated with decreases in the levels of ROS and other markers of oxidative stress [27]. MitoQ was also able to attenuate osteoblast apoptosis caused by advanced glycation end products (AGEs) [28]. Moreover, MitoQ was shown to prevent increased oxidative stress and stimulate mitophagy in a mouse model of periodontitis, both of which are beneficial to bone formation and remodeling [29]. *In vitro* and *in vivo* studies also revealed that MitoQ can effectively reduce mitochondrial oxidative damage caused by erastin-induced ferroptosis and myocardial injury respectively [30, 31].

Considering the beneficial effects observed in various cell types, including those in the skeletal system, with the use of MB or MitoQ, we hypothesized that enhancing mitochondrial function in cells of the osseous system (osteoblasts/osteocytes) during adulthood could serve as a protective measure against age-related bone loss. Our approach included the use of the inbred C57BL6/J mouse strain, one of the most commonly used, extensively characterized, and widely studied strains in scientific research, particularly in the field of biomedical research. In collaboration with The Jackson Laboratory Center for Aging Research, we conducted an experiment where we administered MB to 18-month-old female mice of the C57BL6 strain. We then monitored changes in bone structure for a period of 6 or 12 months after the treatment (Figure 1B). We also employed the genetically diverse UM-HET3 mouse
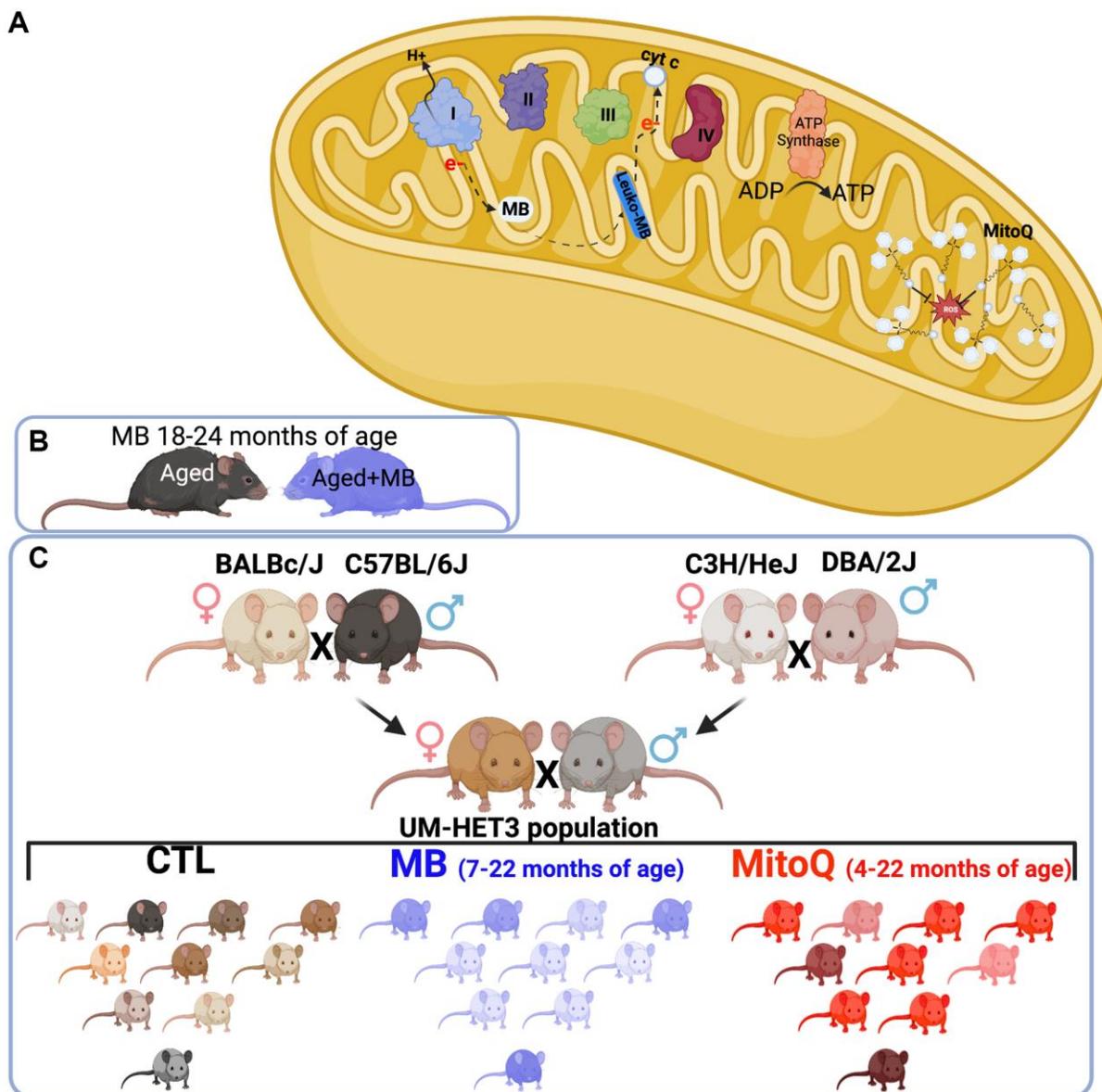

Figure 1. Experimental design. (**A**) Schematic illustration of MB and MitoQ actions in mitochondria. Experimental design of studies both inbred (C57BL/6J) (**B**) and outbred (UM-HET3) (**C**) mouse lines.

strain, which is suitable for studying complex traits, with multifactorial causes, such as skeletal integrity, and is commonly used in aging research. We collaborated with the Interventions Testing Program (ITP), which is supported by the National Aging Institute (NIA), to investigate the effects of lifelong treatment with MB or MitoQ on skeletal structure in genetically diverse UM-HET3 mice (Figure 1C). To assess the skeletal phenotype, we analyzed the appendicular skeleton (specifically the femur) and the axial skeleton (specifically the lumbar vertebra-5) using micro-computed tomography (micro-CT).

RESULTS

Effects of MB and MitoQ on mesenchymal stem cell (MSC) viability, *in vitro* osteogenesis, and mitochondrial respiration in osteoblasts

To investigate the effects of MB and MitoQ on various aspects of osteogenesis, we conducted *in vitro* experiments. Mesenchymal stem cells (MSCs) extracted from femur and tibia of 7-month-old UM-HET3 mice. First, we assessed the effects of increasing concentrations of MB or MitoQ on the viability of MSCs (which includes the osteoprogenitor cell pools). Our results, shown in Supplementary Figure 1, indicated that MSC viability was not significantly affected by doses of 0.125–0.5 µM of MB (Supplementary Figure 1A) or MitoQ (Supplementary Figure 1B). Next, we examined the effect of MB and MitoQ on the differentiation of MSCs to osteoblasts, the bone forming cells. MSCs were induced to differentiate into osteoblasts, in the presence of varying concentrations of MB or MitoQ for 18–28 days. We evaluated the presence of alkaline phosphatase (Alk-Phos) positive colonies as an indicator of osteogenic activity at 18 days of culture. Importantly, no significant differences in Alk-Phos staining were observed between the control group and those treated with MB or MitoQ at concentrations ranging from 0.125–0.5 µM (Figure 2A–2C). To investigate the effects of MB and MitoQ on osteoclast formation, we isolated bone marrow hematopoietic cells and stimulated them with RANKL and M-CSF in the presence of increasing concentrations of MB and MitoQ. Our findings demonstrated that MB and MitoQ inhibited *in vitro* osteoclast differentiation in a dose-dependent manner, as evidenced by a reduced number of multinucleated, TRAP positive cells at concentrations above 0.25 µM (Figure 2D–2F). Additionally, we examined the effect of MB and MitoQ on the respiration of mature osteoblast cells. After 14 days in culture, mature osteoblasts were exposed to different concentrations of MB or MitoQ for 48 hours and then subjected to a mitochondrial stress assay using the Seahorse bioanalyzer. Interestingly, despite their

effects on mitochondrial function, MB or MitoQ did not affect basal oxygen consumption rate (OCR) (Figure 2G–2I) or maximal respiration (Figure 2J) in differentiated osteoblasts.

In summary, our *in vitro* studies indicated that MB and MitoQ did not significantly affect MSC viability or *in vitro* osteogenesis at concentrations ranging from 0.125–0.5 µM. However, these compounds demonstrated dose-dependent inhibition of osteoclast differentiation. Furthermore, 0.5 µM of MB or MitoQ appeared to reduce basal OCR and maximal respiration in differentiated osteoblasts, although these changes were not statistically significant.

Effects of MB on skeletal morphology of the axial and appendicular skeleton of aged female C57BL/6J mice

To investigate the effects of MB on bone morphology during aging, we conducted a study using 18-month-old female C57BL/6J mice. The mice were treated with 250 µM of MB, administered via drinking water for either 6 or 12 months. We dissected bones and tissues at 18, 24, or 30 months of age. Additionally, we included a group of young control females at 5 months of age to evaluate the changes from young to aged mice. The dissected bones were subjected to micro-CT to study bone morphology at three different sites: cortical bone at the femur mid-diaphysis, trabecular bone of the appendicular skeleton at the femur distal metaphysis, and trabecular bone of the axial skeleton at the lumbar vertebra-5 (L5).

Our findings revealed age-associated bone loss at all skeletal sites (Figure 3). In the control females, the total cross-sectional area (T.Ar) increased by 35%, bone area (B.Ar) increased by 24%, and marrow area (M.Ar) increased by 40% from 5 to 18 months of age (data not shown) (Figure 3A, 3B). This resulted in a 10% decrease in the B.Ar/T.Ar ratio between 5 and 18 months of age (Figure 3D). Cortical thickness (C.Th) remained similar between 5 and 18 months of age but decreased by 10% between 18 and 24 months and by 30% between 18 and 30 months of age (Figure 3C). Polar moment of inertia (J0) increased from 5 to 24 months of age and reduced at 30 months (Figure 3E). BMD increased from 5 to 18 months of age in control mice and remained unchanged thereafter (Figure 3F). Mice treated with MB showed similar changes to their corresponding controls at the same age.

At 5 months of age, control females exhibited low levels of trabecular bone volume/total volume (BV/TV) at the distal femur metaphysis, ranging between 5–6% (Figure 4A). Furthermore, we observed decrease in

bone mineral density (BMD) in the trabecular bone compartment at the distal femur, along with decreased trabecular thickness (Tb.Th) with age, regardless of MB treatment (Figure 4B, 4C). However, trabecular number (Tb.N) did not show significant differences with age or treatment (Figure 4D). Similarly, the trabecular bone of the L-5 revealed a 35% reduction in BV/TV, 18% reduction in BMD, and a twofold decrease in Tb.N with age, irrespective of MB treatment (Figure 5A–5C). Tb.Th did not exhibit significant differences between the age or treatment groups (Figure 5D). Overall, MB did not protect against age-induced bone loss.

Muscle and bone are closely interconnected, forming a functional muscle-bone unit. The forces exerted on bones during muscle contractions stimulate bone remodeling, a process that helps maintain bone health [32, 33]. However, with aging muscle strength undergoes changes, which can directly or indirectly affect bone. Indeed, sarcopenia, the age-related loss of muscle mass and strength, has been associated with a decline in bone mineral density and an increased risk of fracture [34]. We did not assess muscle strength in the current study. However, we used grip strength as proxy to measure overall physical function which may only be
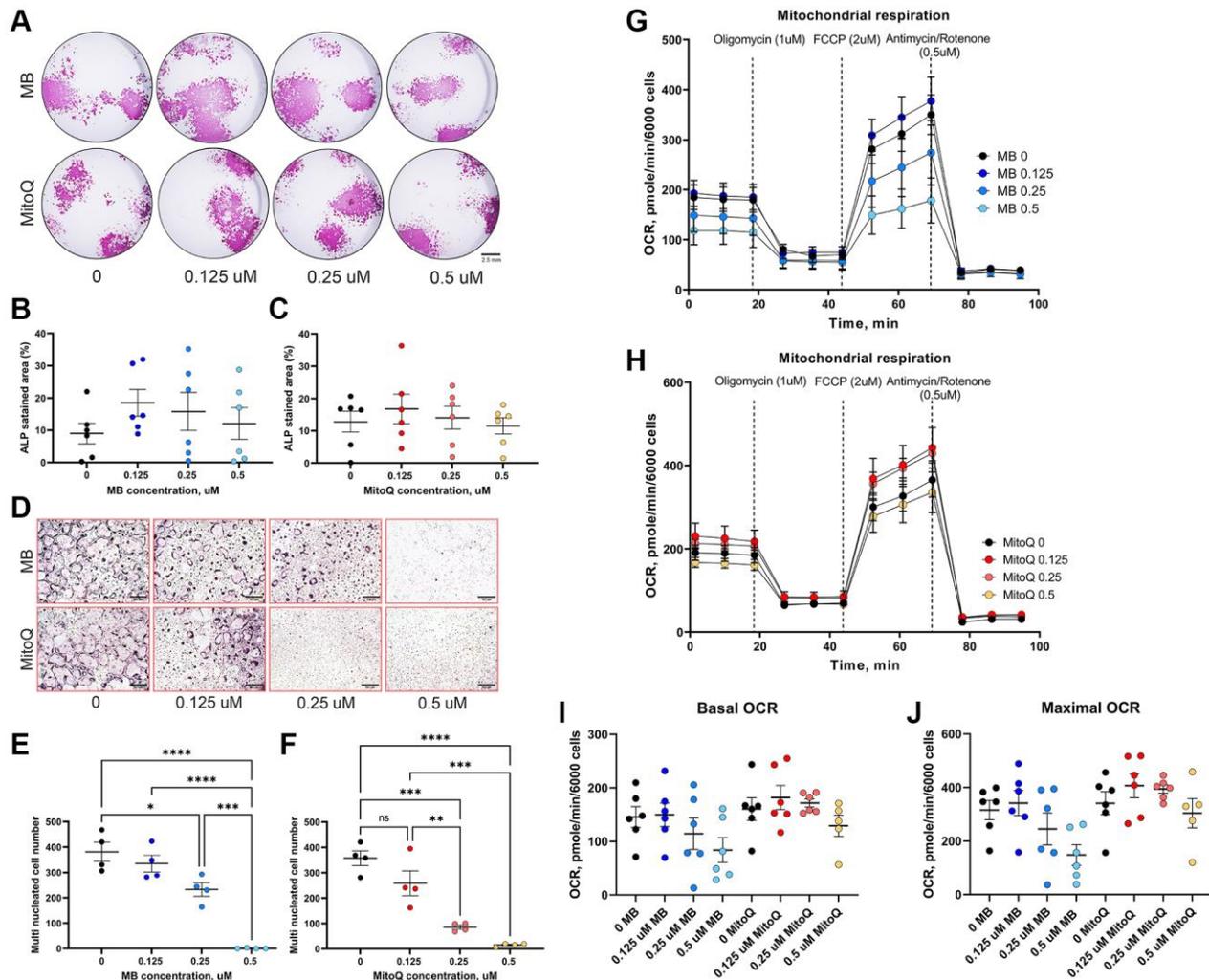

Figure 2. Effects of MB and MitoQ on osteogenesis *in vitro*. BM cells from 6-7 months old UM-HET3 mice were seeded in 24 well plate at a density of 1.5 10^6 cells/well. Adherent cells were subjected for osteoblast differentiation treating with osteogenic factors in the presence or absence of MB or Mito Q at different concentrations (0, 0.125, 025 and 0.5 μM). (**A**) On day 18 in culture, cells were stained for Alkaline-phosphatase (Alk-Phos). The area of Alk-Phos positive colonies treated with (**B**) MB or (**C**) MitoQ were quantified in the wells were measured. (**D**) Non-adherent BM mononuclear cells were separated by Ficoll-Paque density gradient and seeded on 96 wells plate and induced for osteoclast differentiation with the supplementation of RANKL, M-CSF in the presence or absence of (**E**) MB or (**F**) MitoQ (0, 0.125, 025 and 0.5 μM). Multinucleated osteoclasts (>3 nuclei/cell) formed after 5 days in culture were visualized using TRAP staining kit and counted. Differentiated osteoblasts (14 days in culture) were treated with (**G**) MB or (**H**) MitoQ for 48 hours and oxygen consumption rate (OCR) was measured using mitochondrial stress assay kit. (**I**) Basal OCR and (**J**) maximal OCR were recorded along the assay. Data presented as mean ± SEM. We used $n = 6$ mice for assays in A-C, $n = 4$ for assays in D–F, $n = 6$ for mitochondrial stress assay in G–J. Data tested by multivariate ANOVA. Significance accepted at $p < 0.05$ (*$p < 0.05$, **$p < 0.01$, ***$p < 0.001$, ****$p < 0.0001$).

indicative of muscle strength [35]. Previous studies have shown that the administration of 250 μM of MB via drinking water restored the age-related decline in grip strength of 22 months old mice to the levels measured in young mice [36, 37]. However, in our study, despite a noticeable decline in grip strength with age, MB did not affect grip strength (Figure 6A).

Finally, we examined the impact of MB on the expression of genes related to mitochondrial content and function in osteocytes, which are cells embedded within the bone matrix. We observed age-related decreases in the expression of antioxidant enzymes, including catalase-1 and 2, as well as glutathione peroxidase 1 (GPX1). Additionally, the expression of
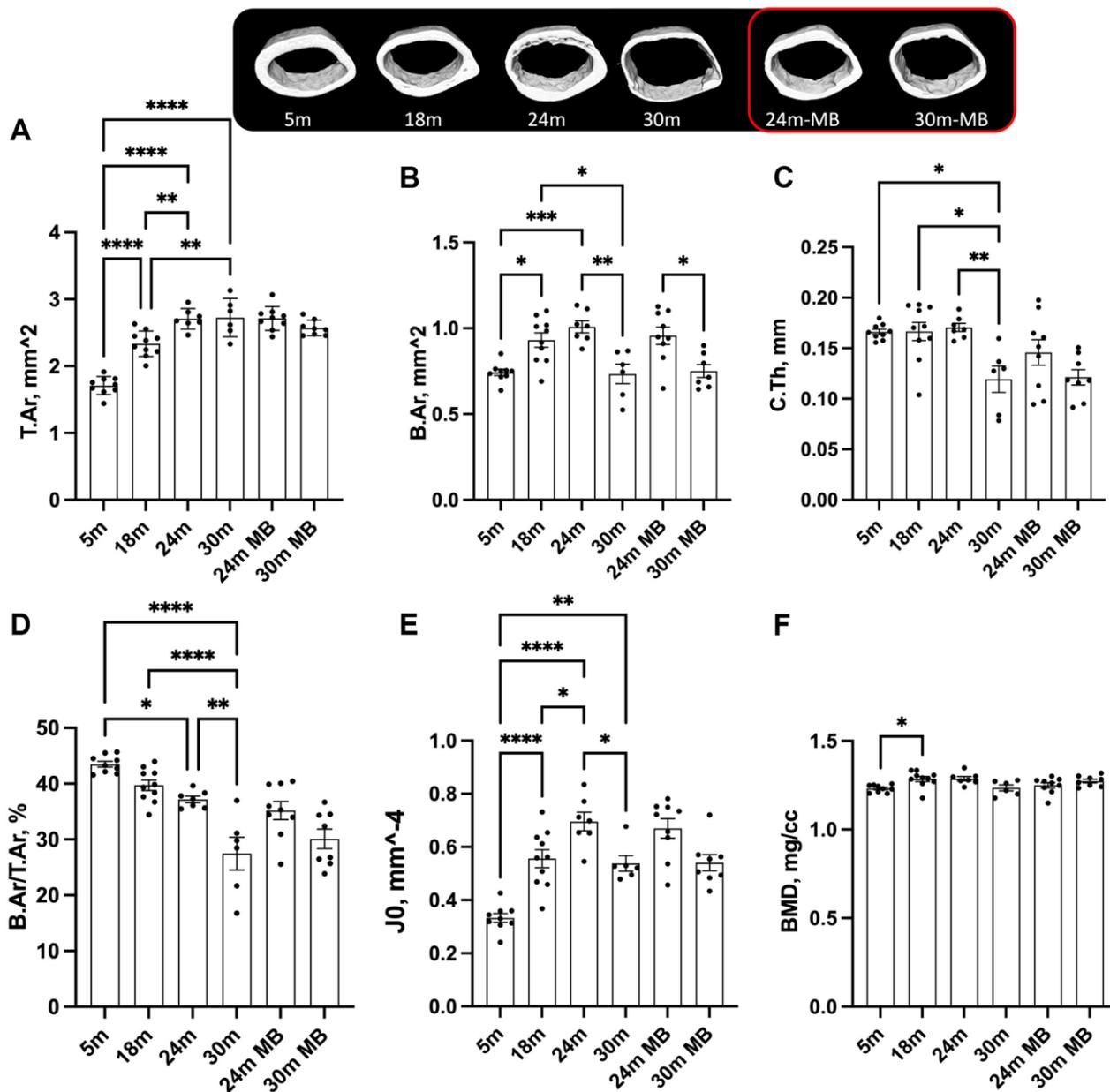

Figure 3. Administration of MB during aging does not alter cortical bone morphology of the appendicular skeleton. Eighteen-months old female C57BL/6J were divided into two groups. One group was exposed to regular drinking water and the other to 250 μM MB-containing water. Mice were sacrificed at basal (18 months), 24, or 30 months of age. An additional group of female mice at 5 months of age, served as young controls. Bones were dissected and subjected to micro-CT. Femurs were scanned at 9.7 um resolution. Cortical bone parameters were evaluated at a 2 mm^3 volume at the femoral mid-diaphysis including, (**A**) T.Ar-total cross-sectional area, (**B**) B.Ar-bone area, (**C**) C.Th-cortical bone thickness, (**D**) B.Ar/T.Ar-cortical bone volume/total volume, (**E**) J0-Polar moment of inertia, and (**F**) BMD-bone mineral density. Data presented as mean ± SEM. 5 months-old females $n = 9$, 18 months-old females $n = 10$, 24 months-old females $n = 7$, 30 months-old females $n = 6$, 24 months-old MB-treated females $n = 9$, 30 months-old MB-treated females $n = 8$. Data tested by multivariate ANOVA presented as mean ± SEM. Significance accepted at $p < 0.05$ (*$p < 0.05$, **$p < 0.01$, ***$p < 0.001$, ****$p < 0.0001$).

mitochondrial markers, such as ATP synthase 6 (ATP6), cytochrome oxidase subunit 1 (Cox1), peroxisome proliferator-activated receptor-g coactivator-1a (PGC1a), and manganese-dependent superoxide dismutase (MnSOD2), were reduced with age. MB did not have a significant effect on the age-related reductions in the expression of these genes (Figure 6B–6H). Notably however, the abundance of the above transcripts can only indicate the potential for protein synthesis and do not directly reflect protein activity.

Effects of MB and MitoQ on skeletal morphology of the axial and appendicular skeleton in UM-HET3 mice

In order to investigate whether early exposure to MB could lead to improved skeletal outcomes, we collaborated with the Interventions Testing Program (ITP). The ITP is a collaborative effort involving three sites: the University of Michigan (UM) led by Richard A. Miller, the Jackson Laboratory (JL) led by David E. Harrison, and the University of Texas Health Science Center at San Antonio (UT) led by John R Strong. This program aims to identify compounds with translational potential to enhance human health-span during aging.

For our study, we utilized the UM-HET3 mouse model, which is genetically heterogeneous. The UM-HET3 mice are derived from a four-way cross involving CByB6F1 females (JAX stock #100009) and C3D2F1 males (JAX stock #100004) (Figure 1C) [38]. This mouse model has been extensively characterized and documented in various publications (https://phenome.jax.org/projects/ITP1). The advantage of the four-way cross is that each offspring shares 50% of its genome with every other offspring in the population, ensuring population-level diversity and reducing the influence of strain-specific traits on the outcomes.

Using the UM-HET3 mice, we examined the effects of two antioxidant interventions, MB and MitoQ, on skeletal morphology. Male and female UM-HET3 mice were treated with MB (28 ppm administered via food) from 7 to 22 months of age, or MitoQ (100 ppm administered via food) from 4 to 22 months of age, along with their respective control groups. We evaluated the morphology of the axial skeleton (L5) and the appendicular skeleton (femur) using micro-CT (Table 1). Long-term administration of MB or MitoQ did not show any significant effects on the skeletal
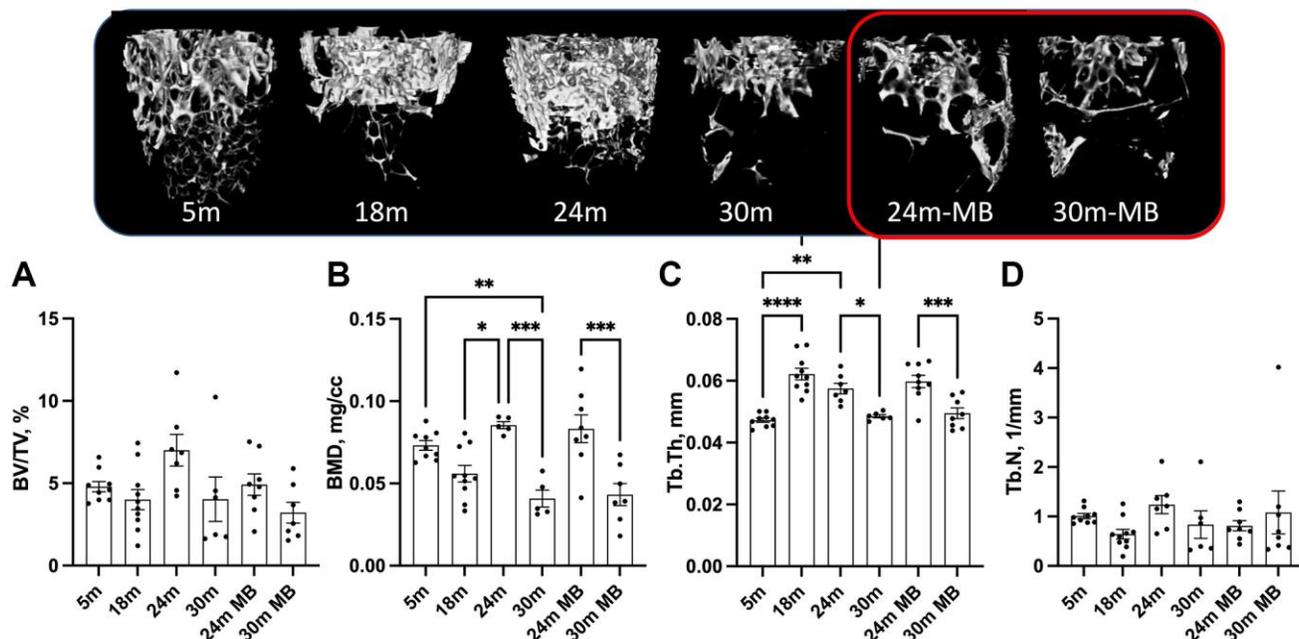

Figure 4. Administration of MB during aging does not alter trabecular bone morphology of the appendicular skeleton. Eighteen-months old female C57BL/6J were divided into two groups. One group was exposed to regular drinking water and the other to 250 µM MB-containing water. Mice were sacrificed at basal (18 months), 24, or 30 months of age. An additional group of female mice at 5 months of age, served as young controls. Bones were dissected and subjected to micro-CT. Femurs were scanned at 9.7 um resolution. Trabecular bone parameters were taken at a 2 mm^3 volume 200 um proximal to the femur distal metaphysis including (**A**) BV/TV-bone volume/total volume, (**B**) BMD-bone mineral density, (**C**) Tb.Th-trabecular thickness, and (**D**) Tb.N-trabecular number. Data presented as mean ± SEM. 5 months-old females $n = 9$, 18 months-old females $n = 10$, 24 months-old females $n = 7$, 30 months-old females $n = 6$, 24 months-old MB-treated females $n = 8$, 30 months-old MB-treated females $n = 7$. Data tested by multivariate ANOVA presented as mean ± SEM. Significance accepted at $p < 0.05$ (*$p < 0.05$, **$p < 0.01$, ***$p < 0.001$, ****$p < 0.0001$).

morphology of aged mice. While we did observe significant sex differences in most bone traits at all skeletal sites, there was no significant effect of treatment or interaction between sex and treatment.

DISCUSSION

The data obtained from the current study suggest that the long-term administration of MB or MitoQ did not have an effect on skeletal morphology during the aging process, even when the treatment was initiated at a young adult age (4 or 7 months-old mice).

Epidemiological studies have provided evidence indicating a relationship between antioxidant intake and bone health. Consequently, numerous studies have been conducted to understand the specific properties of antioxidants and their influence on bone cell metabolism. *In vitro* studies have demonstrated that exposure to peroxide leads to an increase in bone resorption markers, which can be suppressed by the expression of the antioxidant enzyme catalase [39]. Similarly, overexpression of glutathione peroxidase in osteoclast-like RAW-264.7 cells has been shown to suppress osteoclast differentiation [40]. Peroxide has

also been found to inhibit osteoblast differentiation and the formation of type I collagen [41–43]. *In vivo* studies with C57BL/6J mice have shown a progressive loss of BMD in the spine and femur between 4 and 31 months of age, accompanied by decreased bone remodeling, increased apoptosis of osteoblasts and osteocytes, and heightened oxidative stress [44]. Furthermore, the Forkhead Box O (FoxO) transcription factors, which play a role in defense against oxidative stress, have been found to be crucial for skeletal homeostasis [45].

MB and MitoQ were tested in UM-HET3 mice by the ITP [12]. Neither agent led to a significant benefit using the log-rank test, but MB did produce a significant increase, in females, in the proportion of mice alive at the 90th percentile, a surrogate for maximum lifespan (links: MB - https://phenome.jax.org/itp/surv/MB/C2009, MitoQ - https://phenome.jax.org/itp/surv/MitoQ/C2015). In many mouse strains, including C57BL/6J and UM-HET3, tumor progression is the primary cause of death, accounting for 70–90% of all mortality cases [46–51]. Although effects of MB and MitoQ on lifespan appear to be limited, at least at the doses tested by the ITP, these drugs might
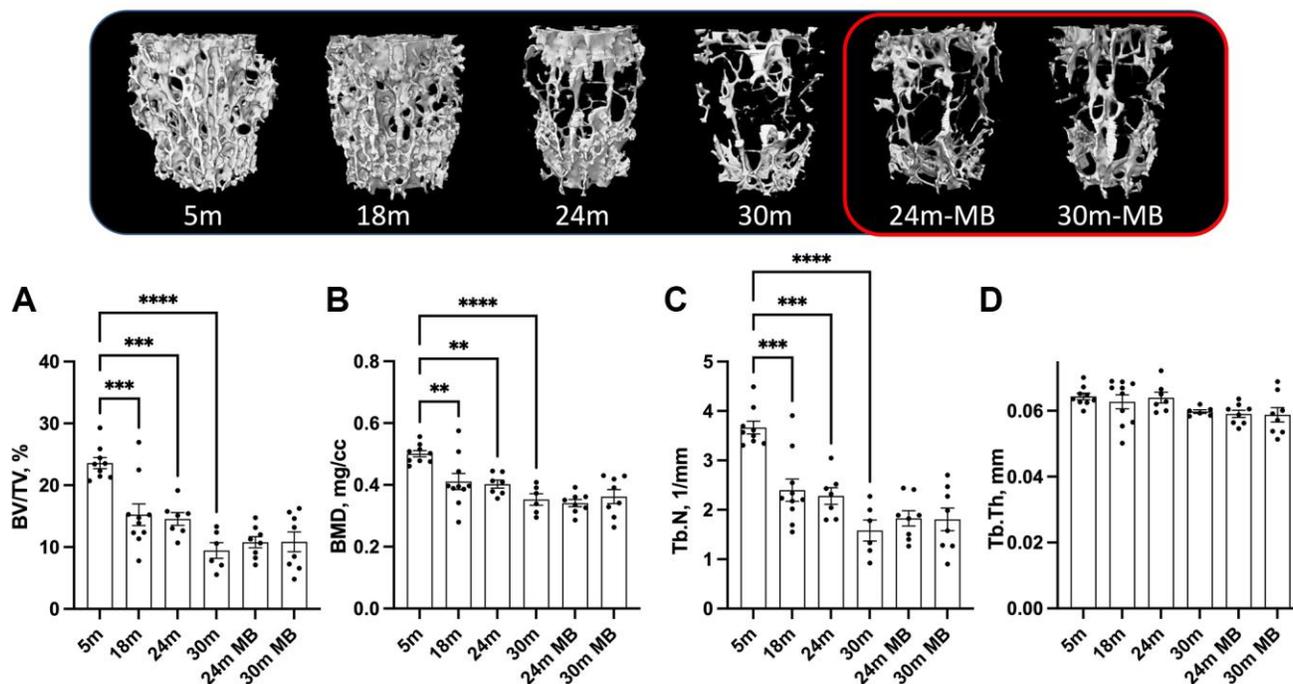

Figure 5. Administration of MB during aging does not alter trabecular bone morphology of the axial skeleton. Eighteen-months old female C57BL/6J were divided into two groups. One group was exposed to regular drinking water and the other to 250 µM MB-containing water. Mice were sacrificed at basal (18 months), 24, or 30 months of age. An additional group of female mice at 5 months of age, served as young controls. Bones were dissected and subjected to micro-CT. Trabecular bone parameters of the L5 vertebra were taken at the vertebral body including, (**A**) BV/TV-bone volume/total volume, (**B**) BMD-bone mineral density, (**C**) Tb.Th-trabecular thickness, and (**D**) Tb.N-trabecular number. 5 months-old females $n = 9$, 18 months-old females $n = 10$, 24 months-old females $n = 7$, 30 months-old females $n = 6$, 24 months-old MB-treated females $n = 8$, 30 months-old MB-treated females $n = 8$. Data tested by multivariate ANOVA presented as mean ± SEM. Significance accepted at $p < 0.05$ ($^*p < 0.05$, $^{**}p < 0.01$, $^{***}p < 0.001$, $^{****}p < 0.0001$).

might in principle have an effect on age-associated bone loss. A recent study that investigated aging trajectories of various phenotypes and molecular markers throughout the lifespan of male C57BL/6J mice indicated that lifespan data alone cannot be used as an indicator for the effects of specific interventions on age-sensitive phenotypes [52]. This was the rationale behind studying the effects of MB and MitoQ interventions on the skeleton despite their limited influence on lifespan.

Sex can have significant implications for how individuals respond to various drug interventions. The physiological and metabolic differences between males and females can influence drug absorption, distribution, metabolism, and excretion. Further, differences in body composition, such as muscle mass and body fat, can influence drug distribution and elimination. Lastly, hormonal variations between sexes can also impact drug metabolism in the liver. However, it's also essential to recognize that not all drugs will necessarily exhibit
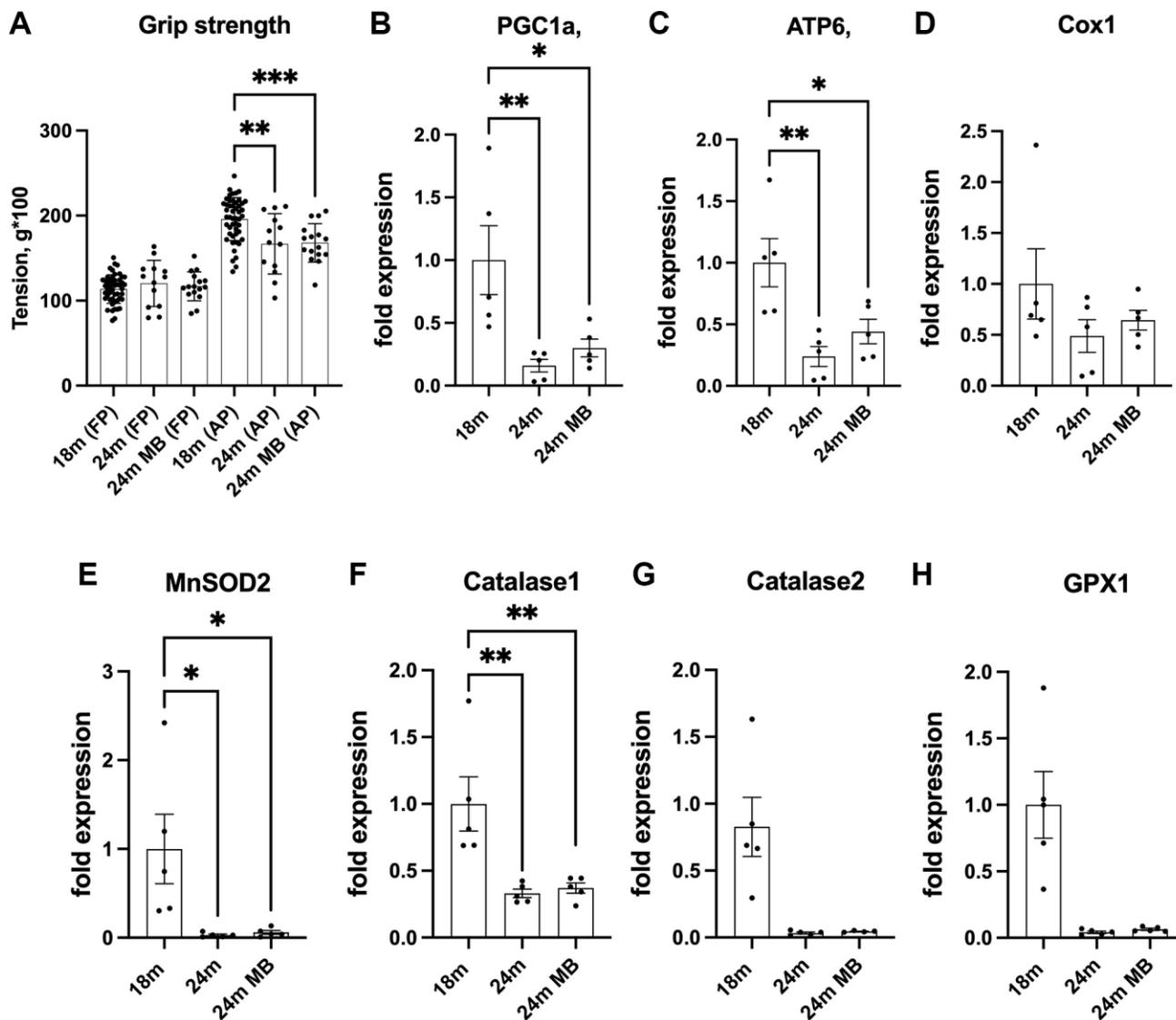

Figure 6. Administration of MB during aging does not affect grip strength or alter skeletal expression of antioxidant enzymes. Eighteen-months old female C57BL/6J were divided into two groups. One group was exposed to regular drinking water and the other to 250 μM MB-containing water for 6 months. (**A**) Grip strength of the front paws (FP) or all four paws (AP) were determined at 18 (basal) and 24 months using the NBP20-16 Grip Strength apparatus. Data presented as a mean value of three consecutive measurements for FP and AP. 18 months-old females $n = 48$, 24 months-old females $n = 13$, 24 months-old BM-treated females $n = 16$. (**B–H**) Gene expression was tested in tibia cortical bone by real-time PCR of 18 months old (basal) and 24 months old mice.- including PGC1a-peroxisome proliferator-activated receptor-g coactivator-1a, ATP6-mitochondrial ATP synthase 6, Cox1-cytochrome oxidase subunit 1, MnSOD2-manganase-dependent superoxide dismutase, Catalase 1, Catalase 2, and GPX1- glutathione peroxidase 1. Data tested by multivariate ANOVA and presented as mean ± SEM of $n = 5$. Significance accepted at $p < 0.05$ ($^*p < 0.05$, $^{**}p < 0.01$, $^{***}p < 0.01$, $^{****}p < 0.0001$).

sex-based differences in their effects, and individual variations can still play a significant role in drug responses. As expected, we found significant sex differences in most bone traits at all skeletal sites in UM-HET3 mice. However, there was no significant effect of treatment or interaction between sex and treatment. Several clinical trials involving MitoQ supplements or MB were registered on ClinicalTrials.gov, but sex-dependent response to those drugs was not reported.

Our study had some limitations, including only using a single dose level of MB or MitoQ, as well as only assessing the skeletal phenotype of the UM-HET3 mice once. Additionally, we did not check on the level of oxidative damage in the bone tissue or cells. Nevertheless, using both inbred (C57BL/6J) and genetically hetero-geneous (UM-HET3) mouse stocks, we did not observe any evidence that either of these antioxidant strategies had positive impacts on bone mineral density or skeletal morphology during ageing. We are not disputing that redox imbalance within bone cells can be a factor in developing bone disease, but rather targeting whole body redox balance via systemic application of MB or MitoQ may not be an effective way to prevent age-related bone loss. We think it may be a better course of action to reduce oxidative stress along the aging process via application of exercise or anabolic bone loading, to protect against age-related decreases in bone health.

METHODS

Animals

Study #1
C57BL/6J female mice: 18 months old C57BL/6J female mice were randomly housed 3–5 in a cage. Mice were housed in a climate-controlled facility with a 12-hour light/dark cycle and provided free access to food and water throughout the experiment. MB (250 µM) was administered via the drinking water. All experiments were approved by The Jackson Laboratory's IACUC.

Study #2
UM-HET3 male and female mice were produced by a cross between (BALB/cByJ × C57BL/6J) F1 mothers (JAX stock #100009) and (C3H/HeJ × DBA/2J)F1 fathers (JAX stock #100004). Detailed housing conditions were specified elsewhere [53]. All experiments were approved by IACUC of each site.

Interventions

Study #1
Mice were fed irradiated Purina TestDiet 5K0G diet and MB (250 µM, Fluka, through Sigma-Aldrich, St. Louis, MO, USA) was administered via the drinking water.

Study #2
MB (28 ppm, starting at 4 months of age) or MitoQ (100 ppm, starting at 7 months of age) were administered in the diet. MB and MitoQ were formulated into irradiated Purina TestDiet 5LG6 diet, and supplied to all three sites so all sites used the same batches of food.

Micro-CT

Micro-CT was done in accordance with the American Society for Bone and Mineral Research (ASBMR) guidelines [54]. Bones were scanned using a high-resolution SkyScan micro-CT system (SkyScan 1172, Kontich, Belgium). Femur were scanned at a 9.7 µm image voxel size. Cortical bone was analyzed in the mid-diaphysis. Trabecular bone measurements were taken at the femur distal metaphysis 200 µm below the growth plate. The 5th lumbar vertebrae (L5) were scanned at a 7.5 µm image voxel size. Image reconstruction was done using NRecon software (version 1.7.3.0; Bruker micro-CT, Kontich, Belgium), data analysis was done using CTAn software (version 1.17.7.2+; Bruker micro-CT, Kontich, Belgium) and 3D images were constructed using CT Vox software (version 3.3.0 r1403; Bruker micro-CT, Kontich, Belgium).

Osteoclast cultures

Bone marrow was flushed out of femur and tibia and cultured over-night in alpha-minimum essential medium (α-MEM, Gibco; cat# 41061-029) containing 10% fetal bovine serum (FBS, Gibco; cat# 10-438-034), 100 U/mL of penicillin-streptomycin (Gibco; cat# 15-140-122) and 0.25 ug/mL amphotericin (Gibco; cat# 15-290-026). Nonadherent cells were removed after 24 h in culture, and subjected to a ficoll (GE Healthcare; cat# 17-1440-03) density gradient. Mononuclear cells were collected and washed with complete medium and 10^4 cells per well in 96 wells plate were plated in the presence of 40 ng/ml M-CSF (Biolegend; cat# 576402) and 60 ng/ml RANKL (R&D Systems; cat# 462TEC010) to induce osteoclastogenesis in the presence of different concentrations (0, 0.125 µM, 0.25 µM and 0.5 µM) of MB or MitoQ. TRAP staining (Sigma-Aldrich; cat# 387A-1K) was done after 5 days in culture, according to manufacturer's instructions.

Bone marrow stromal cell cultures

Bone marrow was flushed out of femur and tibia of 6–7 months old UM-HET3 mice and seeded in α-MEM complete medium. Next day, unattached cells were removed. For a viability assay, cells were collected and seeded in 96 wells plates at the density of 8000 cells per well. Cells were either non-treated (0 µM,

Control) or treated with 0.125 µM, 0.25 µM and 0.5 µM MB or MitoQ. At 48 hours, cells were stained with calcein AM (Invitrogen; cat# C3099) and analyzed using spectrophotometer at excitation and emission of 490 nm and 520 nm wavelengths respectively. For osteogenesis assays, 0.5×10^6 bone marrow cells were plated on 24 wells plate. After a week, cells were induced for osteogenesis with the supplementation of 50 ug/mL of L-ascorbic acid (Sigma -Aldrich; cat# A5960), 10 nm dexamethasone (Sigma -Aldrich; cat# 8893) and 10 mM β-glycero-phosphate in α-MEM complete medium with MB or Mito Q (0, 0.125, 025 and 0.5 µM). The medium was changed twice a week. Alkaline-phosphatase (Alk-Phos) positive cells were assessed on day 18 in culture using Leukocyte Alkaline Phosphatase Kit (Sigma -Aldrich; cat# 86R) following manufacturer instructions.

Mitochondrial stress assay

Primary osteoblast (14 days in culture) was seeded on a type I collagen-coated cell culture micro-plate (4×10^4 cells/well). Cells were treated with different concentrations (0, 0.125, 0.25 and 0.5 µM) of MB or MitoQ for 48 hours and proceed for mitochondrial stress test (Seahorse Bioscience; cat# 101706-100). Accordingly, cells were supplied with 10 mM glucose (Sigma -Aldrich; cat# G7528), 1 mM pyruvate (Sigma -Aldrich; cat# S8636) and 2 mM L-glutamine (Chemicon; cat# TMS-002-C), and oxygen consumption rate (OCR) was determined during basal and upon addition of oligomycin (1 µM), carbonyl cyanide p-(trifluoromethoxy) phenylhydrazone (FCCP, 2 µM) and rotenone/antimycin (0.5 µM) using the Seahorse XFe24 bioanalyzer (Agilent). Data from each well was corrected to cell number using the Bio Tek Cytation 1 Cell Imaging Multimode Reader and presented as mean ± SEM.

Grip strength was tested using the NBP20-16 Grip Strength apparatus (Bioseb). Mice were acclimated to the testing room for a minimum of 60 minutes prior to testing. A mouse was gently lowered towards the wire grid and it instinctively grasped the bar with its paws. Care was taken to ensure the mouse is gripping the grid properly, with both front paws only for forepaw measurements or with all four paws for the combined measurements. Once an appropriate grip was assured, the animal was gently and firmly pulled away from the grid by holding the middle of tail until it releases its grasp. Peak force was measured in g during six consecutive trials. Three consecutive forepaw measurements were followed immediately by three consecutive four paw measurements. Average measurements were calculated for each animal. At the conclusion of testing, mice were returned to their cages. The wire grid was cleaned

with 70% EtOH after each subject, and sanitized with a CMQ-approved agent (e.g., Virkon) at the end of the test session.

Gene expression studies

Total RNA was extracted from tibia cortical shells using TRIzol (Invitrogen, Carlsbad, CA, USA) and RNeasy Plus kit (Cat# 74134, Qiagen). cDNA was generated using a commercial kit (Cat# K1621, Thermo Fisher Scientific). Real-time PCR was done using a BioRad CFX384™ real-time machine with SYBR master mix (Life Technologies/Applied Biosystems, Cat# 4367659). Transcript levels were assayed triplicates and normalized to *beta-actin*. Primer sequences as follows:

ATP6, Forward: 5′-AGCTCACTTGCCCACTTCCT; Reverse: 5′-AAGCCGGACTGCTAATGCCA-3′, beta-actin, Forward: 5′-GGCTGTATTCCCCTCCATCG-3′; Reverse: 5′-CCAGTTGGTAACAATGCCATGT-3′, Catalase 1, Forward: 5′-GCTGAGAAGCCTAAGAAC GC-3′; Reverse: 5′-GTCTCCTCAGCGGAGGCTGA-3′, Catalase 2, Forward: 5′-GCAAGTTCCATTACAAGA CC-3′; Reverse: 5′-CATAATCCGGATCTTCCTGA-3′, Cox1, Forward: 5′-ATCACTACCAGTGCTAGCCG-3′; Reverse: 5′-CCTCCAGCGGGATCAAAGAA-3′, GPX1, Forward: 5′-GTGGTGCTCGGTTTCCCGTGC-3′; Reverse: 5′-CCCGCCACCAGGTCGGACGTA-3′, MnSOD2, Forward: 5′-CTGGCCAAGGGAGATGT TACA-3′; Reverse: 5′-GTCACGCTTGATAGCCTCC AG-3′, and PGC1a, Forward: 5′-TGCAGCGGTCTTA GCACTCA-3′; Reverse: 5′-CATGAATTCTCGGTCT TAACAATGG-3′.

Statistical analyses

Data with inbred (C57BL/6J) mice, presented in Figures 2–6 was tested by multivariant ANOVA presented as mean ± SEM. Significance accepted at $p < 0.05$. Data with genetically heterogeneous (UM-HET3) mice, presented in Table 1. Data presented in Table 1 was tested using 2×2 factorial design for overall data as well as stratified by site and treatment. Outcomes included in the study were first analyzed using nonparametric multivariate analysis of variance with permutation tests (10,000 permutations per outcome). Significant multivariate results were subsequently followed up with two-factor aligned ranks transformation analysis of variance with factors for sex, treatment, and the sex[*] treatment interaction. The false discovery rate for each F-test was controlled for using the method of Benjamini and Hochberg [55]. Finally, *p*-values from post-hoc tests for each significant factor were adjusted using the Bonferroni method. Analysis was conducted in R v4.1.3.

Table 1. Skeletal morphology of 22–24 months old UM-HET3 mice treated with MB or MitoQ.

Treatment	Skeletal site	Parameter	M CTL (*n* = 25)	M MB (*n* = 23)	F CTL (*n* = 24)	F MB (*n* = 25)	Adjusted *P* values		
							Tx	Sex	Tx*Sex
MB	**L5**	BV/TV, %	16.397 ± 7.341	16.485 ± 5.692	11.243 ± 4.674	11.416 ± 5.482	>0.1	**<0.0001**	>0.1
		Tb.Th, mm	0.061 ± 0.008	0.060 ± 0.008	0.062 ± 0.011	0.063 ± 0.007	>0.1	>0.1	>0.1
		Tb.Sp, mm	0.294 ± 0.099	0.282 ± 0.063	0.450 ± 0.082	0.453 ± 0.087	>0.1	**<0.0001**	>0.1
		Tb.N, 1/mm	2.650 ± 1.057	2.712 ± 0.766	1.752 ± 0.532	1.795 ± 0.736	>0.1	**<0.0001**	>0.1
		BMD, g/cm^3	0.394 ± 0.095	0.402 ± 0.081	0.334 ± 0.074	0.336 ± 0.072	>0.1	**0.0009**	>0.1
	Femur mid-diaphysis	B.Ar/T.Ar, %	46.414 ± 9.560	46.803 ± 10.764	51.282 ± 10.277	49.994 ± 11.036	>0.1	>0.1	>0.1
		T.Ar, mm^2	2.462 ± 0.251	2.418 ± 0.508	2.188 ± 0.487	2.256 ± 0.487	>0.1	**0.0039**	>0.1
		B.Ar, mm^2	1.148 ± 0.274	1.118 ± 0.337	1.092 ± 0.285	1.110 ± 0.329	>0.1	>0.1	>0.1
		MMI(polar), mm^{-4}	0.708 ± 0.179	0.707 ± 0.256	0.595 ± 0.194	0.629 ± 0.212	>0.1	**0.049**	>0.1
		Cs.Th, mm	0.204 ± 0.063	0.189 ± 0.059	0.204 ± 0.057	0.199 ± 0.069	>0.1	>0.1	>0.1
		BMD, g/cm^3	1.126 ± 0.145	1.096 ± 0.130	1.141 ± 0.125	1.112 ± 0.152	>0.1	>0.1	>0.1
		Ma.Ar, mm^2	1.314 ± 0.237	1.300 ± 0.311	1.095 ± 0.305	1.146 ± 0.283	>0.1	**0.001**	>0.1
	Femur distal metaphysis	BV/TV, %	5.475 ± 2.861	4.280 ± 2.778	6.195 ± 5.834	6.482 ± 5.742	>0.1	>0.1	>0.1
		Tb.Th, mm	0.063 ± 0.007	0.062 ± 0.010	0.060 ± 0.009	0.065 ± 0.009	>0.1	>0.1	>0.1
		Tb.Sp, mm	0.501 ± 0.188	0.551 ± 0.150	0.709 ± 0.186	0.694 ± 0.169	>0.1	**<0.0001**	>0.1
		Tb.N, 1/mm	0.875 ± 0.453	0.669 ± 0.380	0.978 ± 0.791	0.944 ± 0.705	>0.1	>0.1	>0.1
		BMD, g/cm^3	0.122 ± 0.127	0.089 ± 0.030	0.103 ± 0.055	0.101 ± 0.050	>0.1	>0.1	>0.1

Treatment	Skeletal site	Parameter	M CTL (*n* = 25)	M MitoQ (*n* = 23)	F CTL (*n* = 24)	F MitoQ (*n* = 23)	Tx	Sex	Tx*Sex
MitoQ	**L5**	BV/TV, %	15.353 ± 5.832	14.865 ± 7.369	10.686 ± 3.336	10.677 ± 2.921	>0.1	**0.0014**	>0.1
		Tb.Th, mm	0.059 ± 0.008	0.061 ± 0.013	0.064 ± 0.008	0.062 ± 0.016	>0.1	>0.1	>0.1
		Tb.Sp, mm	0.314 ± 0.141	0.322 ± 0.114	0.459 ± 0.079	0.475 ± 0.120	>0.1	**<0.0001**	>0.1
		Tb.N, 1/mm	2.614 ± 0.922	2.422 ± 1.070	1.685 ± 0.485	1.696 ± 0.464	>0.1	**<0.0001**	>0.1
		BMD, g/cm^3	0.387 ± 0.081	0.385 ± 0.114	0.335 ± 0.051	0.33 ± 0.078	>0.1	**0.0096**	>0.1
	Femur mid-diaphysis	B.Ar/T.Ar, %	44.819 ± 8.153	45.256 ± 11.126	48.544 ± 6.258	50.023 ± 13.127	>0.1	>0.1	>0.1
		T.Ar, mm^2	2.588 ± 0.329	2.458 ± 0.535	2.209 ± 0.233	2.395 ± 0.638	>0.1	**0.0064**	>0.1
		B.Ar, mm^2	1.162 ± 0.259	1.114 ± 0.308	1.071 ± 0.174	1.193 ± 0.317	>0.1	>0.1	>0.1
		MMI(polar), mm^{-4}	0.769 ± 0.237	0.699 ± 0.226	0.573 ± 0.126	0.680 ± 0.195	>0.1	0.06	>0.1
		Cs.Th, mm	0.199 ± 0.046	0.185 ± 0.060	0.215 ± 0.035	0.226 ± 0.062	>0.1	0.0505	>0.1
		BMD, g/cm^3	1.192 ± 0.063	1.206 ± 0.238	1.233 ± 0.055	1.236 ± 0.333	>0.1	**0.0203**	>0.1
		Ma.Ar, mm^2	1.427 ± 0.266	1.344 ± 0.330	1.138 ± 0.193	1.203 ± 0.351	>0.1	**<0.0001**	>0.1
	Femur distal metaphysis	BV/TV, %	3.977 ± 2.025	4.747 ± 2.742	4.696 ± 4.739	4.542 ± 2.870	>0.1	>0.1	>0.1
		Tb.Th, mm	0.062 ± 0.009	0.064 ± 0.015	0.062 ± 0.010	0.062 ± 0.017	>0.1	>0.1	>0.1
		Tb.Sp, mm	0.568 ± 0.198	0.611 ± 0.250	0.776 ± 0.179	0.720 ± 0.179	>0.1	**0.0002**	>0.1
		Tb.N, 1/mm	0.644 ± 0.327	0.739 ± 0.430	0.698 ± 0.598	0.706 ± 0.358	>0.1	>0.1	>0.1
		BMD, g/cm^3	0.092 ± 0.024	0.098 ± 0.033	0.097 ± 0.041	0.098 ± 0.037	>0.1	>0.1	>0.1

Femurs and L5 were scanned using SkyScan 1172 (Microphotonics) at 9.7 or 7.5 um resolution, respectively. Data presented as mean ± SD of mice from the ITP sites. Data tested by descriptive statistics for this 2 × 2 factorial design were computed for overall samples, as well as stratified by site and treatment.

Data availability statement

The datasets generated and analyzed during the current study are all reported. Our studies do not include the use of custom code or mathematical algorithms. We have included citations for available data in the references section.

AUTHOR CONTRIBUTIONS

CONFLICTS OF INTEREST

The authors declare no conflicts of interest related to this study.

ETHICAL STATEMENT

FUNDING

REFERENCES

1. Kimball JS, Johnson JP, Carlson DA. Oxidative Stress and Osteoporosis. J Bone Joint Surg Am. 2021; 103:1451–61.
https://doi.org/10.2106/JBJS.20.00989
PMID:34014853

2. Mainini G, Rotondi M, Di Nola K, Pezzella MT, Iervolino SA, Seguino E, D'Eufemia D, Iannicelli I, Torella M. Oral supplementation with antioxidant agents containing alpha lipoic acid: effects on postmenopausal bone mass. Clin Exp Obstet Gynecol. 2012; 39:489–93.
PMID:23444750

3. Sanders KM, Kotowicz MA, Nicholson GC. Potential role of the antioxidant N-acetylcysteine in slowing bone resorption in early post-menopausal women: a pilot study. Transl Res. 2007; 150:215.
https://doi.org/10.1016/j.trsl.2007.03.012
PMID:17900508

4. Sendur OF, Turan Y, Tastaban E, Serter M. Antioxidant status in patients with osteoporosis: a controlled study. Joint Bone Spine. 2009; 76:514–8.
https://doi.org/10.1016/j.jbspin.2009.02.005
PMID:19464221

5. Marcucci G, Domazetovic V, Nediani C, Ruzzolini J, Favre C, Brandi ML. Oxidative Stress and Natural Antioxidants in Osteoporosis: Novel Preventive and Therapeutic Approaches. Antioxidants (Basel). 2023; 12:373.
https://doi.org/10.3390/antiox12020373
PMID:36829932

6. Domazetovic V, Marcucci G, Iantomasi T, Brandi ML, Vincenzini MT. Oxidative stress in bone remodeling: role of antioxidants. Clin Cases Miner Bone Metab. 2017; 14:209–16.
https://doi.org/10.11138/ccmbm/2017.14.1.209
PMID:29263736

7. Ueno T, Yamada M, Igarashi Y, Ogawa T. N-acetyl cysteine protects osteoblastic function from oxidative stress. J Biomed Mater Res A. 2011; 99:523–31.
https://doi.org/10.1002/jbm.a.33211
PMID:21913320

8. Oliveira CS, Turchiello R, Kowaltowski AJ, Indig GL, Baptista MS. Major determinants of photoinduced cell death: Subcellular localization versus photosensitization efficiency. Free Radic Biol Med. 2011; 51:824–33.
https://doi.org/10.1016/j.freeradbiomed.2011.05.023
PMID:21664269

9. Oz M, Lorke DE, Hasan M, Petroianu GA. Cellular and molecular actions of Methylene Blue in the nervous system. Med Res Rev. 2011; 31:93–117.
https://doi.org/10.1002/med.20177
PMID:19760660

10. Tardivo JP, Del Giglio A, de Oliveira CS, Gabrielli DS, Junqueira HC, Tada DB, Severino D, de Fátima Turchiello R, Baptista MS. Methylene blue in photodynamic therapy: From basic mechanisms to clinical applications. Photodiagnosis Photodyn Ther. 2005; 2:175–91.
https://doi.org/10.1016/S1572-1000(05)00097-9
PMID:25048768

11. Klosowski EM, de Souza BTL, Mito MS, Constantin RP, Mantovanelli GC, Mewes JM, Bizerra PFV, Menezes PVM, Gilglioni EH, Utsunomiya KS, Marchiosi R, Dos Santos WD, Filho OF, et al. The photodynamic and direct actions of methylene blue on mitochondrial energy metabolism: A balance of the useful and harmful effects of this photosensitizer. Free Radic Biol Med. 2020; 153:34–53.
https://doi.org/10.1016/j.freeradbiomed.2020.04.015
PMID:32315767

12. Harrison DE, Strong R, Allison DB, Ames BN, Astle CM, Atamna H, Fernandez E, Flurkey K, Javors MA, Nadon NL, Nelson JF, Pletcher S, Simpkins JW, et al. Acarbose, 17-α-estradiol, and nordihydroguaiaretic

acid extend mouse lifespan preferentially in males. Aging Cell. 2014; 13:273–82.
https://doi.org/10.1111/acel.12170
PMID:24245565

13. Rosenkranz SC, Shaposhnykov AA, Träger S, Engler JB, Witte ME, Roth V, Vieira V, Paauw N, Bauer S, Schwencke-Westphal C, Schubert C, Bal LC, Schattling B, et al. Enhancing mitochondrial activity in neurons protects against neurodegeneration in a mouse model of multiple sclerosis. Elife. 2021; 10:e61798.
https://doi.org/10.7554/eLife.61798
PMID:33565962

14. Pérez MJ, Jara C, Quintanilla RA. Contribution of Tau Pathology to Mitochondrial Impairment in Neurodegeneration. Front Neurosci. 2018; 12:441.
https://doi.org/10.3389/fnins.2018.00441
PMID:30026680

15. Onyango IG, Lu J, Rodova M, Lezi E, Crafter AB, Swerdlow RH. Regulation of neuron mitochondrial biogenesis and relevance to brain health. Biochim Biophys Acta. 2010; 1802:228–34.
https://doi.org/10.1016/j.bbadis.2009.07.014
PMID:19682571

16. Wrubel KM, Riha PD, Maldonado MA, McCollum D, Gonzalez-Lima F. The brain metabolic enhancer methylene blue improves discrimination learning in rats. Pharmacol Biochem Behav. 2007; 86:712–7.
https://doi.org/10.1016/j.pbb.2007.02.018
PMID:17428524

17. Hochgräfe K, Sydow A, Matenia D, Cadinu D, Könen S, Petrova O, Pickhardt M, Goll P, Morellini F, Mandelkow E, Mandelkow EM. Preventive methylene blue treatment preserves cognition in mice expressing full-length pro-aggregant human Tau. Acta Neuropathol Commun. 2015; 3:25.
https://doi.org/10.1186/s40478-015-0204-4
PMID:25958115

18. Paban V, Manrique C, Filali M, Maunoir-Regimbal S, Fauvelle F, Alescio-Lautier B. Therapeutic and preventive effects of methylene blue on Alzheimer's disease pathology in a transgenic mouse model. Neuropharmacology. 2014; 76:68–79.
https://doi.org/10.1016/j.neuropharm.2013.06.033
PMID:23891615

19. Gosain A, DiPietro LA. Aging and wound healing. World J Surg. 2004; 28:321–6.
https://doi.org/10.1007/s00268-003-7397-6
PMID:14961191

20. Xiong ZM, Mao X, Trappio M, Arya C, Kordi JE, Cao K. Ultraviolet radiation protection potentials of Methylene Blue for human skin and coral reef health. Sci Rep. 2021; 11:10871.
https://doi.org/10.1038/s41598-021-89970-2
PMID:34050204

21. Xiong ZM, O'Donovan M, Sun L, Choi JY, Ren M, Cao K. Anti-Aging Potentials of Methylene Blue for Human Skin Longevity. Sci Rep. 2017; 7:2475.
https://doi.org/10.1038/s41598-017-02419-3
PMID:28559565

22. Xiong ZM, Choi JY, Wang K, Zhang H, Tariq Z, Wu D, Ko E, LaDana C, Sesaki H, Cao K. Methylene blue alleviates nuclear and mitochondrial abnormalities in progeria. Aging Cell. 2016; 15:279–90.
https://doi.org/10.1111/acel.12434
PMID:26663466

23. de Oliveira FLD, Nagato AC, Aarestrup FM, Aarestrup BJV. Bone Neoformation Induced by Low-Level Laser and Methylene Blue Suggests Early Ossification in Rats. J Lasers Med Sci. 2022; 13:e48.
https://doi.org/10.34172/jlms.2022.48
PMID:37041788

24. Li JW, Wang RL, Xu J, Sun KY, Jiang HM, Sun ZY, Lv ZY, Xu XQ, Wu R, Guo H, Jiang Q, Shi DQ. Methylene blue prevents osteoarthritis progression and relieves pain in rats via upregulation of Nrf2/PRDX1. Acta Pharmacol Sin. 2022; 43:417–28.
https://doi.org/10.1038/s41401-021-00646-z
PMID:33833406

25. Jiang C, Yang W, Wang C, Qin W, Ming J, Zhang M, Qian H, Jiao T. Methylene Blue-Mediated Photodynamic Therapy Induces Macrophage Apoptosis via ROS and Reduces Bone Resorption in Periodontitis. Oxid Med Cell Longev. 2019; 2019:1529520.
https://doi.org/10.1155/2019/1529520
PMID:31485288

26. James AM, Sharpley MS, Manas AR, Frerman FE, Hirst J, Smith RA, Murphy MP. Interaction of the mitochondria-targeted antioxidant MitoQ with phospholipid bilayers and ubiquinone oxidoreductases. J Biol Chem. 2007; 282:14708–18.
https://doi.org/10.1074/jbc.M611463200
PMID:17369262

27. Li J, He W, Liao B, Yang J. FFA-ROS-P53-mediated mitochondrial apoptosis contributes to reduction of osteoblastogenesis and bone mass in type 2 diabetes mellitus. Sci Rep. 2015; 5:12724.
https://doi.org/10.1038/srep12724
PMID:26226833

28. Mao YX, Cai WJ, Sun XY, Dai PP, Li XM, Wang Q, Huang XL, He B, Wang PP, Wu G, Ma JF, Huang SB. RAGE-dependent mitochondria pathway: a novel target of silibinin against apoptosis of osteoblastic cells induced by advanced glycation end products. Cell Death Dis. 2018; 9:674.

https://doi.org/10.1038/s41419-018-0718-3
PMID:29867140

29. Li X, Zhao Y, Peng H, Gu D, Liu C, Ren S, Miao L. Robust intervention for oxidative stress-induced injury in periodontitis via controllably released nanoparticles that regulate the ROS-PINK1-Parkin pathway. Front Bioeng Biotechnol. 2022; 10:1081977.
https://doi.org/10.3389/fbioe.2022.1081977
PMID:36588945

30. Goh KY, He L, Song J, Jinno M, Rogers AJ, Sethu P, Halade GV, Rajasekaran NS, Liu X, Prabhu SD, Darley-Usmar V, Wende AR, Zhou L. Mitoquinone ameliorates pressure overload-induced cardiac fibrosis and left ventricular dysfunction in mice. Redox Biol. 2019; 21:101100.
https://doi.org/10.1016/j.redox.2019.101100
PMID:30641298

31. Jelinek A, Heyder L, Daude M, Plessner M, Krippner S, Grosse R, Diederich WE, Culmsee C. Mitochondrial rescue prevents glutathione peroxidase-dependent ferroptosis. Free Radic Biol Med. 2018; 117:45–57.
https://doi.org/10.1016/j.freeradbiomed.2018.01.019
PMID:29378335

32. Robling AG, Castillo AB, Turner CH. Biomechanical and molecular regulation of bone remodeling. Annu Rev Biomed Eng. 2006; 8:455–98.
https://doi.org/10.1146/annurev.bioeng.8.061505.095721
PMID:16834564

33. Frost HM. Bone's mechanostat: a 2003 update. Anat Rec A Discov Mol Cell Evol Biol. 2003; 275:1081–101.
https://doi.org/10.1002/ar.a.10119
PMID:14613308

34. Cruz-Jentoft AJ, Baeyens JP, Bauer JM, Boirie Y, Cederholm T, Landi F, Martin FC, Michel JP, Rolland Y, Schneider SM, Topinková E, Vandewoude M, Zamboni M, and European Working Group on Sarcopenia in Older People. Sarcopenia: European consensus on definition and diagnosis: Report of the European Working Group on Sarcopenia in Older People. Age Ageing. 2010; 39:412–23.
https://doi.org/10.1093/ageing/afq034
PMID:20392703

35. Meyer OA, Tilson HA, Byrd WC, Riley MT. A method for the routine assessment of fore- and hindlimb grip strength of rats and mice. Neurobehav Toxicol. 1979; 1:233–6.
PMID:551317

36. Cui L, Hofer T, Rani A, Leeuwenburgh C, Foster TC. Comparison of lifelong and late life exercise on oxidative stress in the cerebellum. Neurobiol Aging. 2009; 30:903–9.
https://doi.org/10.1016/j.neurobiolaging.2007.09.005
PMID:17976863

37. Gharib A, Atamna H. Methylene blue induces mitochondrial complex iv and improves cognitive function and grip strength in old mice. Neurodegeneration: Theory, Disorders and Treatments. 2011; 63–86.

38. Nadon NL, Strong R, Miller RA, Nelson J, Javors M, Sharp ZD, Peralba JM, Harrison DE. Design of aging intervention studies: the NIA interventions testing program. Age (Dordr). 2008; 30:187–99.
https://doi.org/10.1007/s11357-008-9048-1
PMID:19424842

39. Baek KH, Oh KW, Lee WY, Lee SS, Kim MK, Kwon HS, Rhee EJ, Han JH, Song KH, Cha BY, Lee KW, Kang MI. Association of oxidative stress with postmenopausal osteoporosis and the effects of hydrogen peroxide on osteoclast formation in human bone marrow cell cultures. Calcif Tissue Int. 2010; 87:226–35.
https://doi.org/10.1007/s00223-010-9393-9
PMID:20614110

40. Lean JM, Jagger CJ, Kirstein B, Fuller K, Chambers TJ. Hydrogen peroxide is essential for estrogen-deficiency bone loss and osteoclast formation. Endocrinology. 2005; 146:728–35.
https://doi.org/10.1210/en.2004-1021
PMID:15528306

41. Arai M, Shibata Y, Pugdee K, Abiko Y, Ogata Y. Effects of reactive oxygen species (ROS) on antioxidant system and osteoblastic differentiation in MC3T3-E1 cells. IUBMB Life. 2007; 59:27–33.
https://doi.org/10.1080/15216540601156188
PMID:17365177

42. Liu AL, Zhang ZM, Zhu BF, Liao ZH, Liu Z. Metallothionein protects bone marrow stromal cells against hydrogen peroxide-induced inhibition of osteoblastic differentiation. Cell Biol Int. 2004; 28:905–11.
https://doi.org/10.1016/j.cellbi.2004.09.004
PMID:15566960

43. Bai XC, Lu D, Bai J, Zheng H, Ke ZY, Li XM, Luo SQ. Oxidative stress inhibits osteoblastic differentiation of bone cells by ERK and NF-kappaB. Biochem Biophys Res Commun. 2004; 314:197–207.
https://doi.org/10.1016/j.bbrc.2003.12.073
PMID:14715266

44. Almeida M, Han L, Martin-Millan M, Plotkin LI, Stewart SA, Roberson PK, Kousteni S, O'Brien CA, Bellido T, Parfitt AM, Weinstein RS, Jilka RL, Manolagas SC. Skeletal involution by age-associated oxidative stress and its acceleration by loss of sex

steroids. J Biol Chem. 2007; 282:27285–97.
https://doi.org/10.1074/jbc.M702810200
PMID:17623659

45. Ambrogini E, Almeida M, Martin-Millan M, Paik JH, Depinho RA, Han L, Goellner J, Weinstein RS, Jilka RL, O'Brien CA, Manolagas SC. FoxO-mediated defense against oxidative stress in osteoblasts is indispensable for skeletal homeostasis in mice. Cell Metab. 2010; 11:136–46.
https://doi.org/10.1016/j.cmet.2009.12.009
PMID:20142101

46. Xie K, Neff F, Markert A, Rozman J, Aguilar-Pimentel JA, Amarie OV, Becker L, Brommage R, Garrett L, Henzel KS, Hölter SM, Janik D, Lehmann I, et al. Every-other-day feeding extends lifespan but fails to delay many symptoms of aging in mice. Nat Commun. 2017; 8:155.
https://doi.org/10.1038/s41467-017-00178-3
PMID:28761067

47. Brayton CF, Treuting PM, Ward JM. Pathobiology of aging mice and GEM: background strains and experimental design. Vet Pathol. 2012; 49:85–105.
https://doi.org/10.1177/0300985811430696
PMID:22215684

48. Ladiges W. Pathobiology of aging: an old problem gets a new look. Pathobiol Aging Age Relat Dis. 2011; 1.
https://doi.org/10.3402/pba.v1i0.7281
PMID:22953027

49. Miller RA, Harrison DE, Astle CM, Baur JA, Boyd AR, de Cabo R, Fernandez E, Flurkey K, Javors MA, Nelson JF, Orihuela CJ, Pletcher S, Sharp ZD, et al. Rapamycin, but not resveratrol or simvastatin, extends life span of genetically heterogeneous mice. J Gerontol A Biol Sci Med Sci. 2011; 66:191–201.
https://doi.org/10.1093/gerona/glq178
PMID:20974732

50. Lipman R, Galecki A, Burke DT, Miller RA. Genetic loci that influence cause of death in a heterogeneous mouse stock. J Gerontol A Biol Sci Med Sci. 2004; 59:977–83.
https://doi.org/10.1093/gerona/59.10.b977
PMID:15528770

51. Blackwell BN, Bucci TJ, Hart RW, Turturro A. Longevity, body weight, and neoplasia in ad libitum-fed and diet-restricted C57BL6 mice fed NIH-31 open formula diet. Toxicol Pathol. 1995; 23:570–82.
https://doi.org/10.1177/019262339502300503
PMID:8578100

52. Xie K, Fuchs H, Scifo E, Liu D, Aziz A, Aguilar-Pimentel JA, Amarie OV, Becker L, da Silva-Buttkus P, Calzada-Wack J, Cho YL, Deng Y, Edwards AC, et al. Deep phenotyping and lifetime trajectories reveal limited effects of longevity regulators on the aging process in C57BL/6J mice. Nat Commun. 2022; 13:6830.
https://doi.org/10.1038/s41467-022-34515-y
PMID:36369285

53. Strong R, Miller RA, Astle CM, Floyd RA, Flurkey K, Hensley KL, Javors MA, Leeuwenburgh C, Nelson JF, Ongini E, Nadon NL, Warner HR, Harrison DE. Nordihydroguaiaretic acid and aspirin increase lifespan of genetically heterogeneous male mice. Aging Cell. 2008; 7:641–50.
https://doi.org/10.1111/j.1474-9726.2008.00414.x
PMID:18631321

54. Bouxsein ML, Boyd SK, Christiansen BA, Guldberg RE, Jepsen KJ, Müller R. Guidelines for assessment of bone microstructure in rodents using micro-computed tomography. J Bone Miner Res. 2010; 25:1468–86.
https://doi.org/10.1002/jbmr.141
PMID:20533309

55. Benjamini Y, Hochberg Y. Controlling the False Discovery Rate: A Practical and Powerful Approach to Multiple Testing. J R Stat Soc Series B Stat Methodol. 1995; 57:289–300. https://www.jstor.org/stable/2346101.
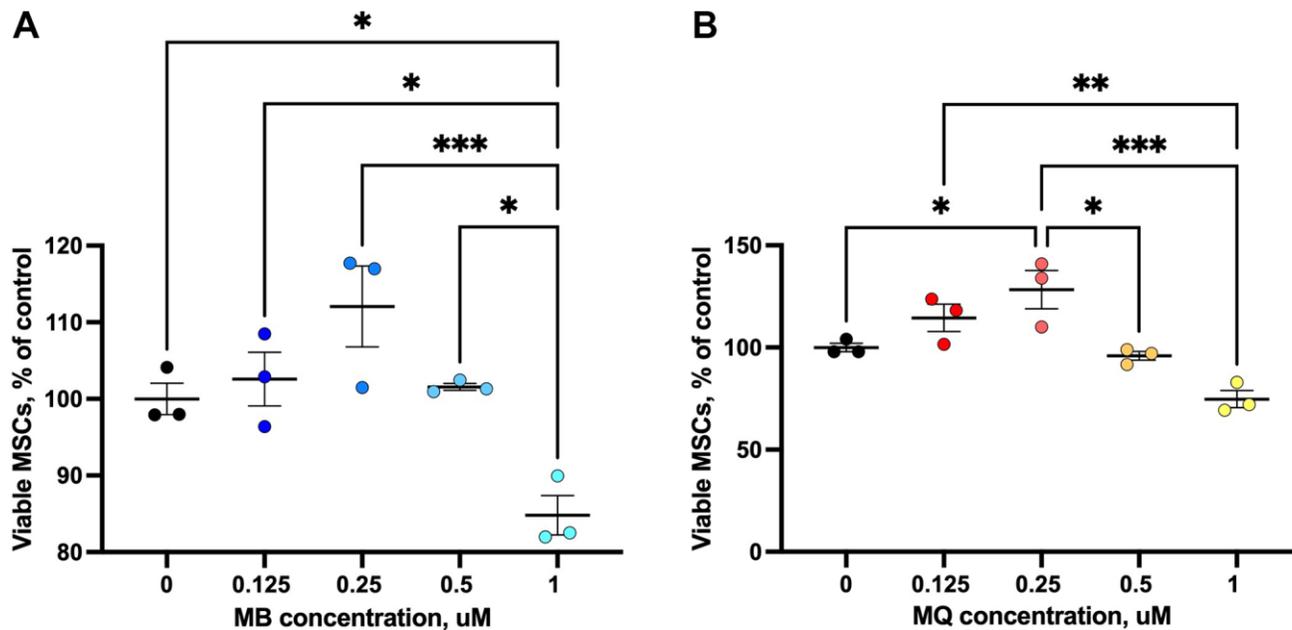
Supplementary Figure 1. Effects of MB or MitoQ on BMSCs viability. BMSCs isolated from 6–7 months were seeded on 96 wells plate in the presence or absence of MB (**A**) or MitoQ (**B**) (0, 0.125, 025, 0.5 μM and 1.0 μM) for 48 hours. Percentage of live cells was determined by calcein AM staining. Data presented as mean ± SEM of n = 3. Data tested by multivariate ANOVA. Significance accepted at $p < 0.05$ ($^*p < 0.05$, $^{**}p < 0.01$, $^{***}p < 0.001$, $^{****}p < 0.0001$).